# Anisotropic magnetic order of the Eu sublattice in single crystals of EuFe_{2−x}Co_{x}As_{2} (x=0,0.2) studied by means of magnetization and magnetic torque

Z. Guguchia, S. Bosma, S. Weyeneth, A. Shengelaya, R. Puzniak, Z. Bukowski, J. Karpinski, and H. Keller

Phys. Rev. B **84**, 144506 — Published 4 October 2011

DOI: 10.1103/PhysRevB.84.144506

# Study of the anisotropic magnetic order of the Eu sublattice in single crystals of $EuFe_{2-x}Co_xAs_2$ ($x$=0, 0.2) by means of magnetization and magnetic torque

Z. Guguchia,* S. Bosma, and S. Weyeneth
*Physik-Institut der Universität Zürich, Winterthurerstrasse 190, CH-8057 Zürich, Switzerland*

A. Shengelaya
*Department of Physics, Tbilisi State University, Chavchavadze 3, GE-0128 Tbilisi, Georgia*

R. Puzniak
*Institute of Physics, Polish Academy of Sciences, Aleja Lotników 32/46, PL-02-668 Warsaw, Poland*

Z. Bukowski and J. Karpinski
*Laboratory for Solid State Physics, ETH Zürich, CH-8093 Zürich, Switzerland*

H. Keller
*Physik-Institut der Universität Zürich, Winterthurerstrasse 190, CH-8057 Zürich, Switzerland*

Here, we present a combination of magnetization and magnetic torque experiments to investigate the magnetic orders in undoped $EuFe_2As_2$ and Co doped $EuFe_{1.8}Co_{0.2}As_2$ single crystals. Although at low temperatures typical results for an antiferromagnetic (AFM) state in $EuFe_2As_2$ were found, our data strongly indicate the occurrence of a canted antiferromagnetic (C-AFM) order of the $Eu^{2+}$ moments between 17 K and 19 K, observed even in the lowest studied magnetic fields. However, unlike in the parent compound, no low-field and low-temperature AFM state of the $Eu^{2+}$ moments was observed in the doped $EuFe_{1.8}Co_{0.2}As_2$. Only a C-AFM phase is present at low fields and low temperatures, with a reduced magnetic anisotropy as compared to the undoped system. We present and discuss for both, $EuFe_2As_2$ and $EuFe_{1.8}Co_{0.2}As_2$, the experimentally deduced magnetic phase diagrams of the magnetic ordering of the $Eu^{2+}$ sublattice with respect to the temperature, the applied magnetic field, and its orientation to the crystallographic axes. It is likely that the magnetic coupling of the Eu and the Fe sublattice is strongly depending on Co doping, having detrimental influence on the magnetic phase diagrams as determined in this work. Their impact on the occurrence of superconductivity with higher Co doping is discussed.

PACS numbers: 74.70.Xa, 75.30.Gw, 75.30.Kz, 75.50.Ee

## I. INTRODUCTION

The discovery of superconductivity in the iron-based pnictides[1] provided a new class of compounds to the high temperature superconductor (HTS) family. Three main groups of these iron-based superconductors are intensively studied: the $R$FeAsO compounds with $R$=La-Gd ('1111'),[1,2] the ternary arsenides $AFe_2As_2$ with $A$=Ba, Sr, Ca, Eu ('122'),[3] and the binary chalcogenides such as $FeSe_{1-x}$ ('11').[4] Similar to the cuprate HTS's, the undoped iron-pnictides are not superconducting (SC) at ambient pressure and undergo a spin-density wave (SDW) transition at high temperatures.[5] The SC state in iron-based compounds can be achieved either under pressure (chemical and hydrostatic)[6–15] or by appropriate charge carrier doping of the parent compounds,[16–18] both accompanied by a suppression of the SDW state.

Here, we focus on $EuFe_2As_2$ which is a particularly interesting member of the ternary system $AFe_2As_2$, since the $A$ site is occupied by a rare earth $Eu^{2+}$ $S$-state (orbital moment $L$=0) ion with a $4f^7$ electronic configuration. $Eu^{2+}$ has a total electron spin $S$=7/2, corresponding to a theoretical effective magnetic moment of 7.94 $\mu_B$. It is the only known member of the '122' family containing $4f$ electrons. In addition to the SDW ordering of the Fe moments at $T_{SDW} \simeq 190$ K, an antiferromagnetic (AFM) order of the $Eu^{2+}$ spins at $T_{AFM} \simeq 19$ K was reported by Mössbauer and susceptibility measurements.[19–21] Recently, neutron diffraction measurements were performed on $EuFe_2As_2$ and the magnetic structure illustrated in Fig. 1 was established.[5] This material exhibits an $A$-type AFM order of the $Eu^{2+}$ moments, *e.g.*, the $Eu^{2+}$ spins align ferromagnetically in the planes, while the planes are coupled antiferromagnetically.[5,22] It was demonstrated that by applying a high enough magnetic field, the $Eu^{2+}$ moments can be realigned ferromagnetically in both the parent compound $EuFe_2As_2$[21,23] as well as in the Co-doped system $EuFe_{2-x}Co_xAs_2$ ($x$=0.22).[24] In addition, neutron diffraction measurements[23] suggested a canted AFM (C-AFM) structure of the $Eu^{2+}$ moments in $EuFe_2As_2$ at intermediate magnetic fields.

Co-substitution may induce superconductivity in $EuFe_{2-x}Co_xAs_2$ with a reentrant behavior of resistivity due to the AFM ordering of the $Eu^{2+}$ spins.[25] Reentrant superconducting behavior was also observed in resistivity experiments on $EuFe_2As_2$ under an applied pressure up to 2.5 GPa.[14,15] However, only above 2.8 GPa, where a valence change of the Eu ions from a divalent magnetic state ($4f^7$, $J$=7/2) to a trivalent nonmagnetic state ($4f^6$, $J$=0) was suggested to occur,[7] a sharp transition to a zero-resistivity state was observed.[14] Bulk superconductivity was also achieved in $EuFe_2As_{2-x}P_x$[7,26] where isovalent P-substitution of the As-site includes chemical pressure in $EuFe_2As_2$. No superconductivity was detected in $EuFe_{2-x}Ni_xAs_2$,[27] while superconductivity with a maximum $T_c \simeq 20$ K was reported for $BaFe_{2-x}Ni_xAs_2$.[28] It was suggested in various reports[21,27,29,30] that there is a strong coupling between the localized $Eu^{2+}$ spins and the conduction electrons of the $Fe_2As_2$ layers. Recently, the hyperfine coupling constant $A_{Eu}$ between the $^{75}$As nuclei and the Eu $4f$ states in $EuFe_{1.9}Co_{0.1}As_2$ was quantitatively determined from $^{75}$As NMR to be $A_{Eu}$=-1.9 $\times$ $10^7$ A/m$\mu_B$.[31] This large value of $A_{Eu}$ indicates a strong coupling between the $Eu^{2+}$ localized moments and the charge carriers in the $Fe_2As_2$ layers and points to a strong correlation between the ordering of the localized magnetic moments and superconductivity in $EuFe_{2-x}Co_xAs_2$.

It is well established that the SDW state of the Fe moments is suppressed as a result of Co doping. However, at present there is no clear picture how the ordering of the Eu spins develops with increasing Co concentration. Generally, it was assumed that in the '122' systems the direction of the sublattice magnetization of the $Eu^{2+}$ magnetic moments is strongly affected by the magnetic behavior of the Fe atoms.[5,32–36] Thus, it is important to compare the magnetic properties of the Eu-sublattice in $EuFe_{2-x}Co_xAs_2$ without and with Co doping in order to study the correlation between ordering of $Eu^{2+}$ moments and the magnetism of the Fe sublattice. This in turn, is crucial to understand the interplay between magnetism of localized moments and supercondcutivity in $EuFe_{2-x}Co_xAs_2$.

In this work, we present magnetic susceptibility, magnetization, and magnetic torque experiment performed on single crystals of $EuFe_{2-x}Co_xAs_2$ ($x$=0, 0.2). The goal of this study is to investigate the macroscopic magnetic properties of the Eu-sublattice. Magnetic susceptibility and magnetization investigations provide information on the magnetic structure of a single-crystal sample in magnetic fields applied along the principal axes. In addition, the evolution of the magnetic structure as a function of the tilting angle of the magnetic field and the crystallographic axis can be studied by magnetic torque. This paper is organized as follows: Experimental details are described in Sec. II. The results of the magnetic susceptibility, the magnetization and the magnetic torque measurements are presented and discussed in Sec. III. In Sec. IV the magnetic phase diagrams of the $Eu^{2+}$ sublattice ordering with respect to magnetic field and temperature in single crystals of $EuFe_{2-x}Co_xAs_2$ ($x$=0, 0.2) are discussed. The conclusions follow in Sec. V.

## II. EXPERIMENTAL DETAILS

Single crystals of $EuFe_{2-x}Co_xAs_2$ ($x$ = 0, 0.2) were grown out of Sn flux.[31] The magnetization measurements of the $EuFe_{2-x}Co_xAs_2$ ($x$ = 0, 0.2) samples were performed with a commercial SQUID magnetometer (*Quantum Design* MPMS-XL) with the magnetic field $H$ applied parallel ($H \parallel c$) or perpendicular ($H \perp c$) to the crystallographic $c$-axis. The magnetic torque measurements were carried out using a home-made torque sensor.[37] The sample is mounted on a platform hanging on piezoresistive legs. A magnetic field $\vec{H}$ applied to the sample having magnetic moment $\vec{m}$ results in a mechanical torque $\vec{\tau} = \mu_0 \vec{m} \times \vec{H}$. This torque bends the legs, and thus creats a measurable electric signal proportional to the torque amplitude. The temperature is controlled by an *Oxford* flow cryostat, and the magnetic field is provided by a rotatable resistive *Bruker* magnet with a maximum magnetic field of 1.4 T.

## III. RESULTS

### A. Magnetization measurements

#### 1. Temperature dependence

The temperature dependence of the magnetic susceptibility $\chi = M/H$ (here $M$ is the magnetization determined as magnetic moment per mol) for the crystal of $EuFe_2As_2$ in a field of $\mu_0 H = 0.01$ T for $H \perp c$ and for $H \parallel c$ is shown in Fig. 2a. In agreement with previous reports,[20,21] the magnetic susceptibility for $H \perp c$ ($\chi_\perp$) and for $H \parallel c$ ($\chi_\parallel$), determined in the temperature range from 30 to 190 K (*i.e.*, far above $T_{AFM} \simeq 19$ K of the Eu moments up to $T_{SDW} \simeq 190$ K of the Fe moments) is well described by the Curie-Weiss law:

$$\chi(T) = \frac{C}{T - \theta_{CW}}. \quad (1)$$

Here, $C$ denotes the Curie constant and $\theta_{\rm CW}$ the Curie-Weiss temperature. Analyzing the data in Fig. 2a with Eq. (1) yields: $C = 1853(15)\times10^{-7}$ m$^3$ K/mol, $\theta_{\rm CW} = 19.74(8)$ K for $H \parallel c$ and $C = 2127(23)\times10^{-7}$ m$^3$ K/mol, $\theta_{\rm CW} = 20.69(4)$ K for $H \perp c$. The calculated effective magnetic moment is $\mu_{\rm eff} \simeq 7.6\ \mu_{\rm B}$ for $H \parallel c$ and $\mu_{\rm eff} \simeq 8.3\ \mu_{\rm B}$ for $H \perp c$. These estimates of $\mu_{\rm eff}$ are close to the theoretical value of the magnetic moment of a free $Eu^{2+}$ ion ($\mu_{\rm Eu^{2+}} = 7.94\ \mu_{\rm B}$). The positive value of $\theta_{\rm CW}$ for both $H \parallel c$ and $H \perp c$ is consistent with previous magnetization measurements,[20,21] indicating that the direct interaction between the $Eu^{2+}$ moments is ferromagnetic (FM). This is in agreement with the magnetic structure of $EuFe_2As_2$ suggested by zero field neutron diffraction measurements,[5] revealing that the intralayer arrangment of the $Eu^{2+}$ spins is FM. The sharp increase of $\chi$ with decreasing temperature below 30 K also indicates a FM coupling between the $Eu^{2+}$ moments. The Eu moments align with respect to the Fe moments along the a axis[5] as illustrated in Fig. 1.

With decreasing temperature from 19 K to 17 K, the susceptibility $\chi_\perp$ of single-crystal $EuFe_2As_2$ decreases rapidly and below 17 K the decrease of $\chi_\perp$ is less pronounced. On the other hand, $\chi_\parallel$ decreases with decreasing temperature from 19 K to 17 K and remains constant below 17 K. Moreover, the values of $\chi_\perp$ and $\chi_\parallel$ at 19 K are substantially different ($\chi_\perp/\chi_\parallel \simeq 1.33$), already in a rather low magnetic field $\mu_0 H = 0.01$ T (see Fig. 2a). Note that within the classical picture of an ideal antiferromagnet, the magnetic susceptibility $\chi$ in a magnetic field perpendicular to the easy axis is constant, and $\chi$ in a field parallel to the easy plane decreases linearly with decreasing temperature. In addition, for an antiferromagnet the values of $\chi$ at the antiferromagnetic (AFM) transition temperature are the same for both $H \perp c$ and $H \parallel c$.[22] The inset of Fig. 2a illustrates the temperature dependence of the difference between both susceptibilities $\chi_{\rm d} = \chi_\perp - \chi_\parallel$. Note that below 19 K the quantity $\chi_{\rm d}$ decreases with decreasing temperature and reaches zero at around 17 K. This behavior of $\chi_{\rm d}(T)$ can be explained by invoking a transition from the high-temperature paramagnetic state to a FM state or to a C-AFM state at about 19 K. The transition from a FM or a C-AFM to an AFM state of the $Eu^{2+}$ spins occurs only below 17 K. The pronounced increase of $\chi_\parallel$ above 17 K indicates the appearence of a magnetic moment along the $c$-axis. Since $\chi_\parallel$ is smaller than $\chi_\perp$ in the FM/C-AFM state, it is suggested that the $ab$-plane is the easy plane of this ordered state. In Fig. 2b the temperature dependences of $\chi_\perp$ and $\chi_\parallel$ of single-crystal $EuFe_2As_2$ in a magnetic field of 0.3 T and 0.5 T (inset) are shown. Obviously, the AFM transition temperatures for $H \perp c$ (crossing point of $\chi_\perp$ and $\chi_\parallel$) and for $H \parallel c$ (temperature at which $\chi_\parallel$ starts to increase) are shifted to lower temperature with higher magnetic field (see Fig. 2a for comparison). However, at $\mu_0 H = 0.5$ T the curves $\chi_\perp$ and $\chi_\parallel$ do not cross in the investigated temperature range, indicating that the AFM state of the $Eu^{2+}$ ions is suppressed in $EuFe_2As_2$ in magnetic fields $H \perp c$ exceeding $\mu_0 H \simeq 0.5$ T. For $H \parallel c$ the suppresion of the AFM state occurs in fields higher than $\mu_0 H \simeq 1.2$ T, since above this field the susceptibility for $H \parallel c$ is temperature dependent even at temperature as low as 2 K (see Fig. 3b). Importantly, the magnetic field at which the magnetic moments of the Eu sublattice saturates (*i.e.*, the field at which the FM state is reached) is much higher than the field of suppresion of the AFM state. This implies that a FM state appears in a magnetic field higher than the field of suppression of antiferromagnetism and that those two transitions are distinguishable. The peak in the magnetic susceptibility at about 19 K in low fields (see Fig. 2) can be associated with the transition from a PM to a C-AFM state. This peak is shifted to lower temperature with applied magnetic field above $\mu_0 H \simeq 0.3$ T for $H \perp c$ and above $\mu_0 H \simeq 0.5$ T for $H \parallel c$ (see Figs. 2b and 3b). Finally, we may conclude that a field-induced magnetic phase transition from an AFM via a C-AFM configuration to a FM state takes place below 17 K. Such a transition is visible even at the lowest temperature of 2 K reached in our experiment.

The magnetization $M(T)$ in the FM state in the vicinity of the Curie temperature $T_{\rm C}$ can be described by the power law:

$$M(T) = M_0 \left(1 - \frac{T}{T_{\rm C}}\right)^{\tilde{\beta}}. \qquad (2)$$

Here $\tilde{\beta}$ and $M_0$ are empirical constants. Analyzing the data at 1.5 T with Eq.(2) yields: $T_{\rm C} = 27.2(1)$ K and $\tilde{\beta} = 0.39(1)$ for both directions of the magnetic field (solid lines in the insets of Fig. 3a and 3b). It was found that $T_{\rm C}$ increases gradually with increasing applied magnetic field for $H \perp c$ and $H \parallel c$. By extrapolating $T_{\rm C}(H)$ to low fields the zero-field value of $T_{\rm C}$ was found to be $\simeq 19$ K. The present values of $T_{\rm C}(H)$ are in agreement with those reported by Xiao *et al.*[23]

The temperature dependence of the magnetic susceptibility for the Co doped crystal $EuFe_{1.8}Co_{0.2}As_2$ in an applied field of $\mu_0 H = 0.01$ T for $H \perp c$ and $H \parallel c$ is presented in Fig. 4. In the inset the temperature dependence of the difference between the susceptibilities for two field configurations $\chi_{\rm d} = \chi_\perp - \chi_\parallel$ is shown. Analyzing the susceptibility data above 30 K with Eq. (2) yields: $C = 2108(32)\times10^{-7}$ m$^3$ K/mol, $\theta_{\rm CW} = 21.86(6)$ K for $H \perp c$ and $C = 1915(34)\times10^{-7}$ m$^3$ K/mol, $\theta_{\rm CW} = 20.67(7)$ K for $H \parallel c$. Again $\theta_{\rm CW}$ turns out to be positive. Like in the parent compound a sharp increase of $\chi$ below 30 K is observed, which is attributed to the in-plane FM coupling between the $Eu^{2+}$ moments. Below 17 K the susceptibility $\chi_\perp$ starts to decrease with decreasing temperature, indicating the onset of an AFM transition of the $Eu^{2+}$ spins. On the other hand, $\chi_\parallel$ remains almost constant below 17 K. This

suggests that the $Eu^{2+}$ moments align along the *ab*-plane, similar to undoped $EuFe_2As_2$. However, for $EuFe_2As_2$ the AFM ordering temperature of the $Eu^{2+}$ spins is about 2 K higher. Below 17 K, $\chi_\perp$ is significantly larger than $\chi_\parallel$, even in magnetic fields as low as $\mu_0 H$=0.01 T (see Fig. 4). Thus, no crossing between $\chi_\perp$ and $\chi_\parallel$ is observed (inset of Fig. 4), in contrast to the parent compound $EuFe_2As_2$ (see Fig. 2). Furthermore, $\chi_\perp$ is temperature dependent even at the lowest applied magnetic field. This is inconsistent with an AFM state with an easy *c*-axis. Hence, we suggest that for all temperatures below 17 K the ground state of the coupled $Eu^{2+}$ spins in $EuFe_{1.8}Co_{0.2}As_2$ is a C-AFM state with a FM component in the *ab*-plane. This implies that the magnetic configuration of the Eu moments is strongly influenced by the magnetization of the Fe-sublattice. This is consistent with previous NMR studies, revealing a strong coupling between the Eu and $Fe_{2-x}Co_xAs_2$ layers.[31]

The temperature dependences of $\chi_\perp$ and $\chi_\parallel$ at different magnetic fields of single-crystal $EuFe_{1.8}Co_{0.2}As_2$ are shown in Fig. 5. Zero field cooling (ZFC) and field cooling (FC) susceptibilities $\chi_\perp(T)$ measured in an applied field of $\mu_0 H$ = 0.001 T are shown in the inset of Fig. 5a. Below 17 K the ZFC and FC curves deviate from each other, indicating the presence of a C-AFM state of the $Eu^{2+}$ moments. The data reveal a decrease of the C-AFM ordering temperature $T_{\mathrm{C-AFM}}$ with increasing magnetic field for both field orientations, similar as for the parent compound $EuFe_2As_2$. However, the values for $T_{\mathrm{C-AFM}}$ for $EuFe_{1.8}Co_{0.2}As_2$ are substantially smaller than those for $EuFe_2As_2$.

#### *2. Field dependence*

The susceptibility investigations of the previous section clearly demonstrate that the system $EuFe_{2-x}Co_xAs_2$ ($x$ = 0, 0.2) shows a rich variety of magnetic phases. In order to explore in detail the various magnetic field-induced phases, magnetization experiments were also performed as a function of the applied magnetic field at different temperatures.

The field dependence of the magnetization of single-crystal $EuFe_2As_2$ at different temperatures for $H \perp c$ is shown in Fig. 6. In the inset the low field magnetization $M_\perp$ at 5 K is shown. $M_\perp$ increases almost linearly with increasing magnetic field $H$ up to $\mu_0 H \simeq 0.45$ T where a sudden increase of $M_\perp$ appears. Then $M_\perp$ further increases with increasing $H$, and finally saturates for $\mu_0 H \geq 0.8$ T. The value of the saturation magnetization corresponds to an effective magnetic moment of 6.8 $\mu_B$/f.u., which is close to $g\mu_B S = 7$ $\mu_B$/f.u. expected for $Eu^{2+}$ moments. This result suggests that there is a metamagnetic (MM)[38,39] transition at $\mu_0 H_{\mathrm{MM}} \simeq 0.45$ T at 5 K in $EuFe_2As_2$, consistent with previous observations.[20,21] Such a metamagnetic transition is characteristic for A-type antiferromagnetism in layered systems as, *e.g.*, $Na_{0.85}CoO_2$[38] and $La_{2-x}Sr_{1+x}Mn_2O_7$.[40] Figure 6 shows that the MM transition shifts towards lower fields with increasing temperature. The values of the magnetic field at which the MM transition occurs is in agreement with the results obtained from the susceptibility for the AFM to C-AFM transition. Thus, we propose that the MM transition corresponds to the onset of a spin-flop transition[22] from an AFM to a C-AFM state in $EuFe_2As_2$. However, no MM transition for $H \perp c$ is detected in $EuFe_{1.8}Co_{0.2}As_2$ (Fig. 7a). Both $M_\perp$ and $M_\parallel$ first increase almost linearly with increasing $H$ and then saturate at higher fields (Fig. 7). The absence of a MM transition in $EuFe_{1.8}Co_{0.2}As_2$ is consistent with the susceptibility measurements presented above, suggesting that the $Eu^{2+}$ moments exhibit a C-AFM ground state even at very low $H$. This conclusion is also supported by magnetic hysteresis measurements at 5 K performed in magnetic fields up to 0.5 T. As demonstrated in the inset of Fig. 7a the field dependence of $M_\perp$ at 5 K shows a well developed hysteresis for $EuFe_{1.8}Co_{0.2}As_2$, in contrast to the parent compound $EuFe_2As_2$ where no hysteresis is observed.

Obviously, the presented susceptibility and magnetization measurements reveal a complex and rather sophisticated interplay of magnetic phases in the $EuFe_{2-x}Co_xAs_2$ system. Additional information on the complex magnetic phases in $EuFe_{2-x}Co_xAs_2$ is obtained from angular dependent magnetic torque studies presented in the next section.

### B. Magnetic torque

In low magnetic fields the $Eu^{2+}$ magnetic moments prefer to order antiferromagnetically in $EuFe_2As_2$. High magnetic fields reorient the magnetic moments, leading to various magnetic field induced phases. Magnetic torque allows to investigate multiple aspects of magnetic order as a function of the magnetic field with respect to the principal axes. Whereas magnetization provides direct information on the magnetic moment oriented along the field, magnetic torque directly probes the anisotropy of the susceptibility in magnetic systems.

The angular dependence of the magnetic torque $\tau$ of single-crystal $EuFe_2As_2$ measured at 13 K in various magnetic fields is presented in Fig. 8a. In Fig. 8b the same data are plotted in terms of $\tau/(\mu_0 H^2)$. The torque data below 0.3 T are of sinusoidal shape, following a simple angular dependence for a uniaxial antiferromagnet:[41]

$$\tau(\theta) = -V \frac{(\chi_\perp - \chi_\parallel)}{2} \mu_0 H^2 \sin(2\theta). \quad (3)$$

Here, $\theta$ denotes the angle between the field $H$ and the crystallographic $c$-axis, $V$ is the volume of the sample, and $\chi_\perp$ and $\chi_\parallel$ are the magnetic susceptibilities for $H \perp c$ and for $H \parallel c$, respectively. Above 0.3 T the shape of the torque signal changes drastically (see Fig. 8). For $\theta \simeq 90°$($H$ almost parallel to the $ab$-plane) an additional torque signal appears, with an opposite sign relative to the AFM torque. Upon increasing the magnetic field this additional signal rises steeply and leads to a sign change of the torque signal for all angles $\theta$. A similar behavior was observed in $RbVBr_3$[42] and was interpreted as the appearance of a weak field-induced magnetic moment. This additional contribution to the torque signal observed here is substantially larger than the AFM torque signal. This is consistent with the magnetization data (see Sec. III(A)), from which the presence of a C-AFM phase was concluded above 0.3 T at 13 K. The sign change of the torque signal is in agreement with the sign change of the quantity $\chi_\mathrm{d} = \chi_\perp - \chi_\parallel$, which was interpreted as a signature of a transition to a C-AFM state of the $Eu^{2+}$ magnetic moments. It was shown previously[29] that $EuFe_2As_2$ exhibits a weak in-plane anisotropy. Since the in-plane anisotropy is much weaker than the out-of-plane anisotropy, this system can be treated approximately as a uniaxial anisotropic antiferromagnet. However, even a small in-plane anisotropy may lead to discrepancies between experimental results and theoretical predictions for a uniaxial anisotropic ferromagnet. Particularly, the torque signal of the AFM state shown in Fig. 8a is shifted by $\Delta\theta \sim 10°$ with respect to one of the C-AFM state (see Fig 8b). A similar phase shift $\Delta\theta$ was observed in $\lambda$ - $(BETS)_2FeCl_4$[43] and interpreted as a change of the easy-axis. However, here the phase shift appears to indicate a crystallographic multi-domain state, due to a twinning of the crystal in the AFM state.

Figure 9a shows the measured magnetic torque for the same $EuFe_2As_2$ single crystal at 20 K, where according to the magnetization results the AFM regime has disappeared. Consistently, no AFM torque signal is observed. Instead, the magnetic torque amplitude increases with $H^2$ and saturates at higher $H$. Such a behavior is characteristic for a paramagnet. Consistently, the quantity $\tau/(\mu_0 H^2)$ plotted in in Fig. 9b decreases with increasing field.

In Fig. 10 the scaled magnetic torque $\tau/(\mu_0 H^2)$ for $EuFe_2As_2$ and $EuFe_{1.8}Co_{0.2}As_2$ is shown in a color map for the representative temperatures of 13 K, 17 K, and 20 K as a function of angle $\theta$ and field $H$. Note that $\tau/(\mu_0 H^2)$ is scaling according to the magnetic susceptibility. As seen in Fig. 10a the low field regime of undoped $EuFe_2As_2$ at 13 K is dominated by the AFM state, whereas for higher fields, the C-AFM state appears abruptly along a clearly angular dependent boundary line (dotted line), demonstrating the anisotropy of this magnetically ordered system. At 17 K (Fig. 10b) the AFM phase is not present, consistent with the conclusions from the above susceptibility measurements. At 20 K (Fig. 10c) the signal is clearly sinusoidal, consistent with FM behavior. In order to induce the canting of a planar antiferromagnetically ordered subsystem, the in-plane component of the magnetic field $H_\perp$ must surpass a threshold value $H_{\mathrm{cant},\perp}$. In order to induce a canting of a planar antiferromagnetically ordered subsystem, the in-plane component of the magnetic field $H_\perp$ must overcome the in-plane magnetization $\mathcal{M}_\perp$ in one of the two magnetic sublattices:

$$H_\perp \geqslant A \cdot \mathcal{M}_\perp = A \cdot \sqrt{\mathcal{M}^2 - \mathcal{M}_\parallel^2}. \tag{4}$$

Here, $\mathcal{M}$ is the saturation magnetization of the magnetic sublattice, $\mathcal{M}_\parallel$ its out-of-plane component, and $A$ is a constant. Taking into account

$$\begin{aligned} H_\perp &= H\sin(\theta), \\ \mathcal{M}_\parallel &= \frac{1}{2}\chi_\parallel H\cos(\theta), \end{aligned} \tag{5}$$

where $\chi_\parallel$ is the suceptibility of the total $Eu^{2+}$ magnetic sublattice, we obtain for the boundary condition:

$$H^2\sin^2(\theta) = A^2\left(\mathcal{M}^2 - \frac{1}{4}\chi_\parallel^2 H^2\cos^2(\theta)\right). \tag{6}$$

Solving this equality for $H$ yields the angle dependent canting field:

$$H_\mathrm{cant}(\theta) = \frac{A\cdot\mathcal{M}}{\sqrt{\sin^2(\theta) + \frac{1}{4}\chi_\parallel^2 A^2\cos^2(\theta)}}. \tag{7}$$

Interestingly, the resulting $H_\mathrm{cant}(\theta)$ is analog to the expression for the angular dependence of the upper critical field $H_{c2}(\theta)$ in a type II superconductor.[44] Hence, Eq. (7) can be simplified according to

$$H_\mathrm{cant}(\theta) = \frac{H_{\mathrm{cant},\perp}}{\sqrt{\sin^2(\theta) + \gamma_\mathrm{cant}^{-2}\cos^2(\theta)}}, \tag{8}$$

where $H_{\mathrm{cant},\perp} = H_{\mathrm{cant}}(90°)$ is the in-plane canting field, $\gamma_{\mathrm{cant}} = H_{\mathrm{cant},\parallel}/H_{\mathrm{cant},\perp}$ its anisotropy parameter, and $H_{\mathrm{cant},\parallel} = H_{\mathrm{cant}}(0°)$ the out-of-plane canting field. This shape of the angular dependence of the transition between the AFM and C-AFM phase in the ($H$, $\theta$) diagram is represented by the dashed line in Fig. 10a. It describes the experimental torque data rather well, with the parameters $H_{\mathrm{cant},\perp}(13\ \mathrm{K}) \simeq 0.42(2)$ T and $\gamma_{\mathrm{cant}} \simeq 2.0(2)$. This yields an estimate of the canting field parallel to the $c$-axis $H_{\mathrm{cant},\parallel}(13\ \mathrm{K}) \simeq 0.84(6)$ T.

The low field torque signal of $EuFe_{1.8}Co_{0.2}As_2$ at 20 K (Fig. 10f) shows a shape typical for an anisotropic paramagnet. However, the anisotropy of the system is quite quickly suppressed with increasing magnetic field, which may indicate a transformation of the paramagnetic state to a short range ordered state at relatively low field. It might be caused by large fluctuations of the magnetic moments in the vicinity of the transition from a disordered PM state to an ordered one in $EuFe_{1.8}Co_{0.2}As_2$. Furthermore, at low temperatures we do not observe any indication of a field induced transition from the AFM to the C-AFM state (Fig. 10d-e). Therefore, we conclude that for $EuFe_{1.8}Co_{0.2}As_2$ even at the lowest magnetic field a transition from a PM to a C-AFM state takes place with decreasing temperature, in agreement with the above magnetization data.

## IV. DISCUSSION

In Fig. 11 the results of the susceptibility, magnetization, and magnetic torque experiments are summarized. They are discussed in terms of the phase diagram of the $Eu^{2+}$ magnetic sublattice of $EuFe_2As_2$ and $EuFe_{1.8}Co_{0.2}As_2$ for $H \perp c$ and $H \parallel c$.

### A. $EuFe_2As_2$

For the parent compound $EuFe_2As_2$ four different magnetic phases were identified (see Fig. 11a and b): a paramagnetic (PM), an antiferromagnetic (AFM), a canted antiferromagnetic (C-AFM), and a ferromagnetic (FM) phase. The determination of the corresponding transition temperatures and fields is described in Sec. III. The present experiments suggest a C-AFM order of the $Eu^{2+}$ spins in $EuFe_2As_2$ in the temperature range between 17 K and 19 K, while below 17 K an AFM structure is proposed. We suggest that at low temperatures the system can be well described with a uniaxial model with easy plane and A-type AFM order. By applying a magnetic field within the AFM phase, a transition from AFM order via a canted configuration to a FM structure is observed. The observed $T_{\mathrm{MM}}(H)$ at which the metamagnetic (MM) transition occurs (open symbols in Fig. 11a) is in agreement with the results obtained from the susceptibility for the AFM to C-AFM transition (black filled symbols in Fig. 11a). Thus, we propose that the MM transition corresponds to a spin-flop transition from an AFM to a C-AFM state in $EuFe_2As_2$. The critical magnetic field $H_{\mathrm{cr}}(T)$ at which the magnetic moment in the Eu sublattice saturates was determined at different temperatures. The values of $H_{\mathrm{cr}}$ extrapolated to zero temperature were found to be $\mu_0 H_{\mathrm{cr},\perp}(0) \simeq 0.85$ T and $\mu_0 H_{\mathrm{cr},\parallel}(0) \simeq 1.5$ T for $H \perp c$ and $H \parallel c$, respectively. By analyzing the shape of the angular dependence of $H_{\mathrm{cr}}(\theta)$ shown in Fig. 10a, we may conclude that the in-plane component of the magnetic field is responsible for the canting of the spins.

The magnetic ordering of the $Eu^{2+}$ moments at low temperatures is consistent with the magnetic structure established by neutron diffraction at 2.5 K.[5] Note that in previous reports[20,21] a possible C-AFM state in the temperature range 17 K $\leq T \leq$ 19 K was not discussed. To our knowledge no neutron data for the magnetic configuration of the Eu sublattice in this temperature range is available.

### B. $EuFe_{1.8}Co_{0.2}As_2$

The corresponding magnetic phase diagrams for Co-doped $EuFe_{1.8}Co_{0.2}As_2$ are shown in Fig. 11c and d. The magnetic ordering temperature of $\simeq 17$ K is only about 2 K lower as compared to the parent compound. However, in the Co-doped $EuFe_{1.8}Co_{0.2}As_2$, no signatures of a low-field and low-temperature AFM state of the $Eu^{2+}$ moments was found. Only a C-AFM phase (with a FM component in the $ab$-plane) is present at low fields and low temperatures. The ordering temperature $T_{\mathrm{C-AFM}}$ decreases with increasing magnetic field, similar to the parent compound (see Fig. 11a and b). The critical magnetic field $H_{\mathrm{cr}}$ at which the Eu magnetic ordering is saturated was determined for different temperatures, and the extrapolated zero-temperature values were found to be: $\mu_0 H_{\mathrm{cr},\perp}(0) \simeq 0.43$ T and $\mu_0 H_{\mathrm{cr},\parallel}(0) \simeq 0.58$ T for $H \perp c$ and $H \parallel c$, respectively. These values of $\mu_0 H_{\mathrm{cr}}$ are much smaller than those obtained for the parent compound. Moreover, the magnetic anisotropy $\gamma_{\mathrm{cr}} = H_{\mathrm{cr},\parallel}(0)/H_{\mathrm{cr},\perp}(0) \simeq 1.35$ of Co-doped $EuFe_{1.8}Co_{0.2}As_2$ is also smaller than $\gamma_{\mathrm{cr}} \simeq 1.76$ of the parent compound.

It was concluded from different experiments[21,27,29–31] that there is a strong coupling between the localized $Eu^{2+}$ spins and the conduction electrons of the two-dimensional (2D) $Fe_2As_2$ layers. Recently, direct experimental evidence

for a strong interlayer coupling was obtained by means of $^{75}$As NMR,[31] revealing a magnetic exchange interaction between the localized Eu $4f$ moments which is mediated by the itinerant Fe $3d$ electrons. However, the direct interaction of the Eu moments and the magnetic moments in Fe sublattice cannot be neglected. Only a combination of both interactions can further elucidate the C-AFM ground state observed in the parent compound $EuFe_2As_2$ as well as in the Co-doped system $EuFe_{1.8}Co_{0.2}As_2$ (see Fig. 11).

Note that the present results for $EuFe_{1.8}Co_{0.2}As_2$, exhibiting a SDW ground state below 60 K,[30] reveal a C-AFM structure of the Eu spins with a FM component in the *ab*-plane. This finding confirms previous assumptions that for materials in which the Fe ions are in the SDW ground state (such as $EuFe_2As_2$) the direction of the Eu magnetic moments is in the *ab*-plane.[5,32] On the other hand, in the case of non-magnetic Fe ground states, like in superconducting $EuFe_{2-x}Co_xAs_2$ compounds, where the SDW magnetic state is totally suppresed, the direction of the Eu magnetic moments is parallel to the *c*-axis.[33–36]

## V. CONCLUSIONS

The magnetic properties of single crystals of $EuFe_2As_2$ and $EuFe_{1.8}Co_{0.2}As_2$ were studied by means of susceptibility, magnetization, and magnetic torque investigations. The susceptibility and magnetization experiments performed for various temperatures and magnetic fields along the crystallographic axes provided information on the magnetic structure of the studied crystals. In addition, the evolution of the magnetic structure as a function of the tilting angle of the field and the crystallographic axes is studied by magnetic torque experiments. The phase diagrams for the ordering of the $Eu^{2+}$ magnetic sublattice with respect to temperature, magnetic field and the angle between the magnetic field and the crystallographic *c*-axis in $EuFe_{2-x}Co_xAs_2$ are determined and discussed. The present investigations reveal a complex and sophisticated interplay of magnetic phases in $EuFe_{2-x}Co_xAs_2$. The magnetic ordering temperature of the $Eu^{2+}$ moments remains nearly unchanged upon Co-doping. However, unlike the parent compound, in which the $Eu^{2+}$ moments order antiferromagnetically at low temperatures, the Co-doped system $EuFe_{1.8}Co_{0.2}As_2$ exhibits a C-AFM state with a FM component in the *ab*-plane. The magnetic anisotropy $\gamma_{cr}$ becomes smaller as a result of Co-doping. This implies that the magnetic configuration of the Eu moments is strongly influenced by the magnetic moments of the Fe-sublattice, where superconductivity takes place for a certain range of Co-doping. A detailed knowledge of the interplay between the $Eu^{2+}$ moments and magnetism of the Fe sublattice is important to understand the role of magnetism of the localized $Eu^{2+}$ moments for the occurence of supercondcutivity in $EuFe_{2-x}Co_xAs_2$.

## VI. ACKNOWLEDGMENTS

This work was supported by the Swiss National Science Foundation, the SCOPES grant No. IZ73Z0_128242, the NCCR Project MaNEP, the EU Project CoMePhS, and the Georgian National Science Foundation grant GNSF/ST08/4-416.

* Electronic address: zurabgug@physik.uzh.ch

[1] Y. Kamihara, T. Watanabe, M. Hirano, and H. Hosono, J. Am. Chem. Soc. **130**, 3296 (2008).
[2] X.H. Chen, T. Wu, G. Wu, R.H. Liu, H. Chen, and D.F. Fang, Nature (London) **453**, 761 (2008).
[3] M. Rotter, M. Tegel, and D. Johrendt, Phys. Rev. Lett. **101**, 107006 (2008).
[4] F.-C. Hsu, J.-Y. Luo, K.-W. Yeh, T.-K. Chen, T.-W. Huang, P. M. Wu, Y.-C. Lee, Y.-L. Huang, Y.-Y. Chu, D.-C. Yan, and M.-K. Wu, Proc. Natl. Acad. Sci. USA **105**, 14263 (2008).
[5] Y. Xiao, Y. Su, M. Meven, R. Mittal, C.M.N. Kumar, T. Chatterji, S. Price, J. Persson, N. Kumar, S.K. Dhar, A. Thamizhavel, and Th. Brueckel, Phys. Rev. B **80**, 174424 (2009).
[6] M.S. Torikachvili, S.L. Bud'ko, N. Ni, and P.C. Canfield, Phys. Rev. Lett. **101**, 057006 (2008).
[7] Liling Sun, Jing Guo, Genfu Chen, Xianhui Chen, Xiaoli Dong, Wei Lu, Chao Zhang, Zheng Jiang, Yang Zou, Suo Zhang, Yuying Huang, Qi Wu, Xi Dai, Yuanchun Li, Jing Liu, and Zhongxian Zhao, Phys. Rev. B **82**, 134509 (2010).
[8] H. Lee, E. Park, T. Park, V.A. Sidorov, F. Ronning, E.D. Bauer, and J.D. Thompson, Phys. Rev. B **80**, 024519 (2009).
[9] P.L. Alireza, Y.T.C. Ko, J. Gillett, G.G. Lonzarich, and S.E. Sebastian, J. Phys.: Condens. Matter **21**, 012208 (2009).
[10] K. Igawa, H. Okada, H. Takahahsi, S. Matsuishi, Y. Kamihara, M. Hirano, H. Hosono, K. Matsubayashi, and Y. Uwatoko, J. Phys. Soc. Jpn. **78**, 025001 (2009).
[11] H. Fukazawa, N. Takeshita, T. Yamazaki, K. Kondo, K. Hirayama, Y. Kohori, K. Miyazawa, H. Kito, H. Eisaki, and A. Iyo, J. Phys. Soc. Jpn. **77**, 105004 (2008).

[12] W.J. Duncan, O.P. Welzel, C. Harrison, X.F. Wang, X.H. Chen, F.M. Grosche, and P.G. Niklowite, J. Phys.: Condens. Matter **22**, 052201 (2010).
[13] A. Mani, N. Ghosh, S. Paulraj, A. Bharathi, and C.S. Sundar, Europhys. Lett. **87**, 17004 (2009).
[14] T. Terashima, M. Kimata, H. Satsukawa, A. Harada, K. Hazama, S. Uji, H.S. Suzuki, T. Matsumoto, and K. Murata, J. Phys. Soc. Jpn. **78**, 083701 (2009).
[15] C.F. Miclea, M. Nicklas, H.S. Jeevan, D. Kasinathan, Z. Hossain, H. Rosner, P. Gegenwart, C. Geibel, and F. Steglich, Phys. Rev. B **79**, 212509 (2009).
[16] Z.A. Ren, W. Lu, J. Yang, W. Yi, X.L. Shen, Z.C. Li, G.C. Che, X.L. Dong, L.L. Sun, F. Zhou, and Z.X. Zhao, Chin. Phys. Lett. **25**, 2215 (2008).
[17] S. Matsuishi, Y. Inoue, T. Nomura, M. Hirano, and H. Hosono, J. Phys. Soc. Jpn. **77**, 113709 (2008).
[18] J. Zhao, Q. Huang, C. de la Cruz, S. Li, J.W. Lynn, Y. Chen, M.A. Green, G.F. Chen, G. Li, Z. Li, J.L. Luo, N.L. Wang, and P. Dai, Nature Materials **7**, 953 (2008).
[19] H. Raffius, M. Mörsen, B.D. Mosel, W. Müller-Warmuth, W. Jeitschko, L. Terbüchte, and T. Vomhof, J. Phys. Chem. Solids **54**, 135 (1993).
[20] Z. Ren, Z.W. Zhu, S. Jiang, X.F. Xu, Q. Tao, C. Wang, C.M. Feng, G.H. Cao, and Z.A. Xu, Phys. Rev. B **78**, 052501 (2008).
[21] S. Jiang, Y.K. Luo, Z. Ren, Z.W. Zhu, C. Wang, X.F. Xu, Q. Tao, G.H. Cao, and Z.A. Xu, New J. Phys. **11**, 025007 (2009).
[22] S. Blundell, *Magnetism in Condensed Matter* (New York: Oxford University Press, 2006).
[23] Y. Xiao, Y. Su, W. Schmidt, K. Schmalzl, C.M.N. Kumar, S. Price, T. Chatterji, R. Mittal, L.J. Chang, S. Nandi, N. Kumar, S.K. Dhar, A. Thamizhavel, and Th. Brueckel, Phys. Rev. B **81**, 220406 (2010).
[24] Shuai Jiang, Hui Xing, Guofang Xuan, Zhi Ren, Cao Wang, Zhu-an Xu, and Guanghan Cao, Phys. Rev. B **80**, 184514 (2009).
[25] Y. He, T. Wu, G. Wu, Q.J. Zheng, Y.Z. Liu, H. Chen, J.J. Ying, R.H. Liu, X.F. Wang, Y.L. Xie, Y.J. Yan, J.K. Dong, S.Y. Li, and X.H. Chen, J. Phys.: Condens. Matter **22**, 235701 (2010).
[26] H.S. Jeevan, Deepa Kasinathan, H. Rosner, and P. Gegenwart, Phys. Rev. B **83**, 054511 (2011).
[27] Zhi Ren, Xiao Lin, Qian Tao, Shuai Jiang, Zengwei Zhu, Cao Wang, Guanghan Cao, and Zhu'an Xu, Phys. Rev. B **79**, 094426 (2009).
[28] L.J. Li, Y.K. Luo, Q.B. Wang, H. Chen, Z. Ren, Q. Tao, Y.K. Li, X. Lin, M. He, Z.W. Zhu, G.H. Cao, and Z.A. Xu, New J. Phys. **11**, 025008 (2009).
[29] E. Dengler, J. Deisenhofer, H.A. Krug von Nidda, Seunghyun Khim, J.S. Kim, Kee Hoon Kim, F. Casper, C. Felser, and A. Loidl, Phys. Rev. B **81**, 024406 (2010).
[30] J.J. Ying, T. Wu, Q.J. Zheng, Y. He, G. Wu, Q.J. Li, Y.J. Yan, Y.L. Xie, R.H. Liu, X.F. Wang, and X.H. Chen, Phys. Rev. B **81**, 052503 (2010).
[31] Z. Guguchia, J. Roos, A. Shengelaya, S. Katrych, Z. Bukowski, S. Weyeneth, F. Murányi, S. Strässle, A. Maisuradze, J. Karpinski, and H. Keller, Phys. Rev. B **83**, 144516 (2011).
[32] I. Nowik and I. Felner, *Hyperfine Interact.* **28**, 959 (1986).
[33] I. Nowik and I. Felner, *Physica* C **469**, 485 (2009).
[34] C. Feng, Z. Ren, S. Xu, S. Jiang, Z. Xu, G. Cao, I. Nowik, I. Felner, K. Matsubayashi, and Y. Uwatoko, Phys. Rev. B **82**, 094426 (2010).
[35] I. Nowik, I. Felner, Z. Ren, G.H. Cao, and Z.A. Xu, J. Phys.: Condens. Matter **23**, 065701 (2011).
[36] I. Nowik, I. Felner, Z. Ren, G.H. Cao, and Z.A. Xu, New J. Phys. **13**, 023033 (2011).
[37] S. Kohout, J. Roos, and H. Keller, Rev. Sci. Instrum. **78**, 013903 (2007).
[38] J.L. Luo, N.L. Wang, G.T. Liu, D. Wu, X.N. Jing, F. Hu, and T. Xiang, Phys. Rev. Lett. **93**, 187203 (2004).
[39] R.S. Perry, L.M. Galvin, S.A. Grigera, L. Capogna, A.J. Schofield, A.P. Mackenzie, M. Chiao, S.R. Julian, S.I. Ikeda, S. Nakatsuji, Y. Maeno, and C. Pfleiderer, Phys. Rev. Lett. **86**, 2661 (2001).
[40] T. Kimura and Y. Tokura, Ann. Rev. Mater. Sci. **30**, 451 (2000).
[41] S. Weyeneth, P.J.W. Moll, R. Puzniak, K. Ninios, F.F. Balakirev, R.D. McDonald, H.B. Chan, N.D. Zhigadlo, S. Katrych, Z. Bukowski, J. Karpinski, H. Keller, B. Batlogg, and L. Balicas, Phys. Rev. B **83**, 134503 (2011)
[42] H. Tanaka, T. Kato, K. Iio, and K. Nagata, J. Phys. Soc. Jap. **61**, 3292 (1992).
[43] T. Sasaki, H. Uozaki, S. Endo, and N. Toyota, Synth. Metals **120**, 759 (2001).
[44] V. L. Ginzburg and L. D. Landau, Zh. Eksp. Teor. Fiz. **20**, 1064 (1950).

**Figures**

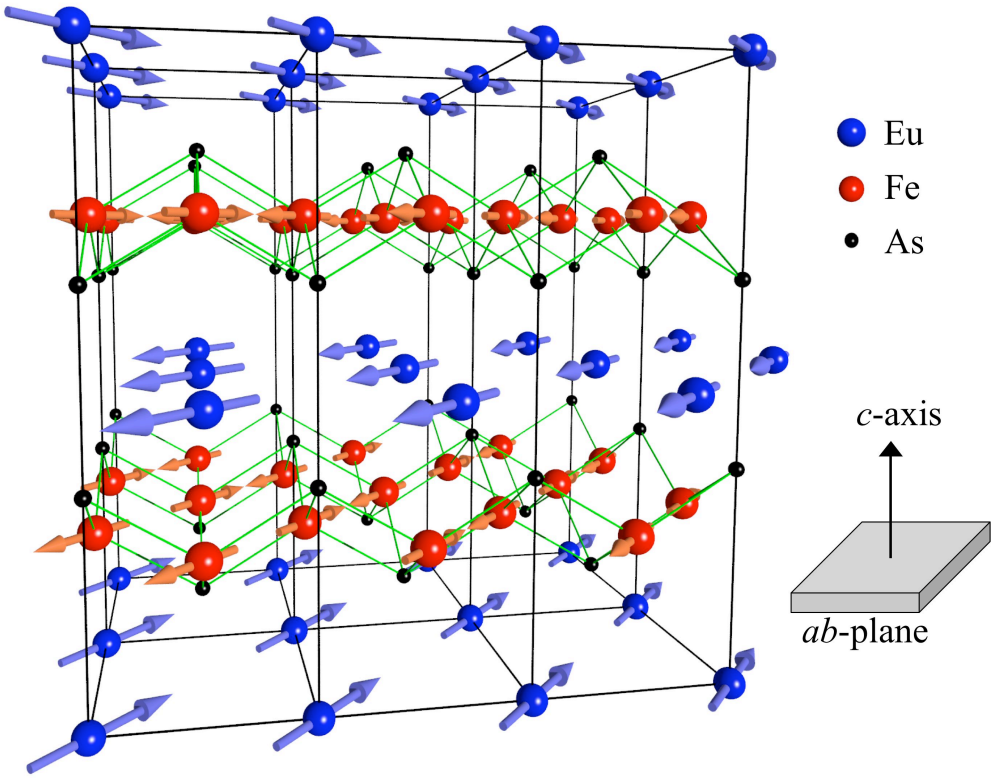


FIG. 1: (Color online) Schematic illustration of the magnetic structure of $EuFe_2As_2$. The Fe moments (red) form a SDW state, whereas the Eu moments (blue) order ferromagnetically in the *ab*-plane and align antiferromagnetically along the *c*-axis.

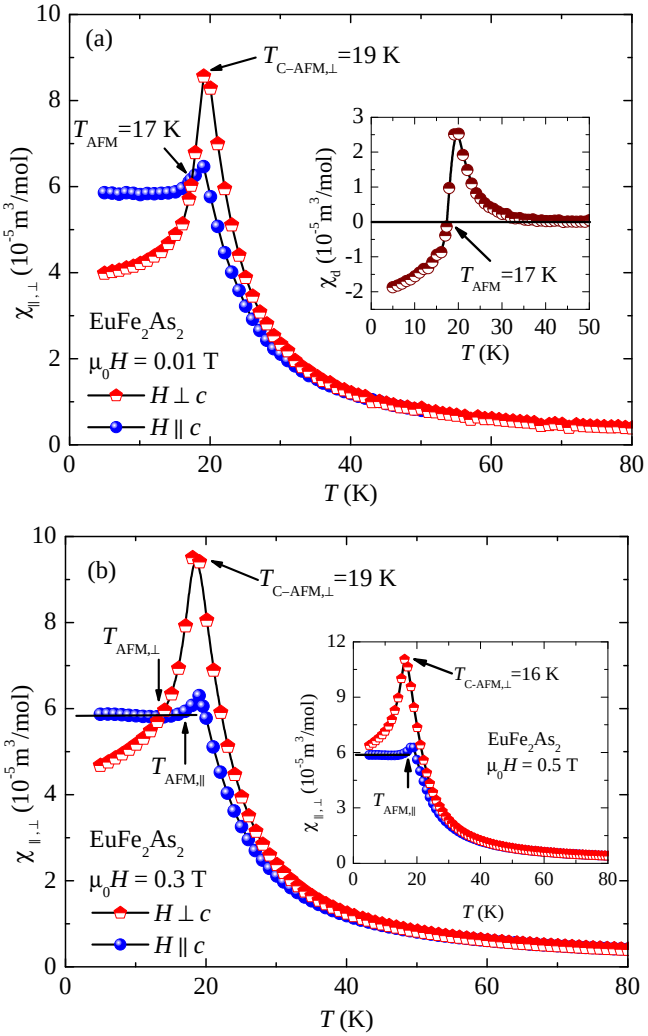


FIG. 2: (Color online) Temperature dependence of the magnetic susceptibility measured at fixed magnetic fields applied perpendicular ($H \perp c$) and parallel ($H \parallel c$) to the crystallographic $c$-axis of single-crystal $EuFe_2As_2$: (a) $\mu_0 H = 0.01$ T; (b) $\mu_0 H = 0.3$ T and $\mu_0 H = 0.5$ T (inset). The inset of panel (a) illustrates the temperature dependence of the difference between both susceptibilities ($\chi_d = \chi_\perp - \chi_\parallel$). The arrows mark the AFM and C-AFM ordering temperatures of the $Eu^{2+}$ moments, and $T_{AFM,\perp}$ and $T_{AFM,\parallel}$ refer to the AFM ordering temperatures for $H \perp c$ and $H \parallel c$, respectively. The canted-AFM ordering temperature for $H \perp c$ is denoted by $T_{C-AFM,\perp}$.

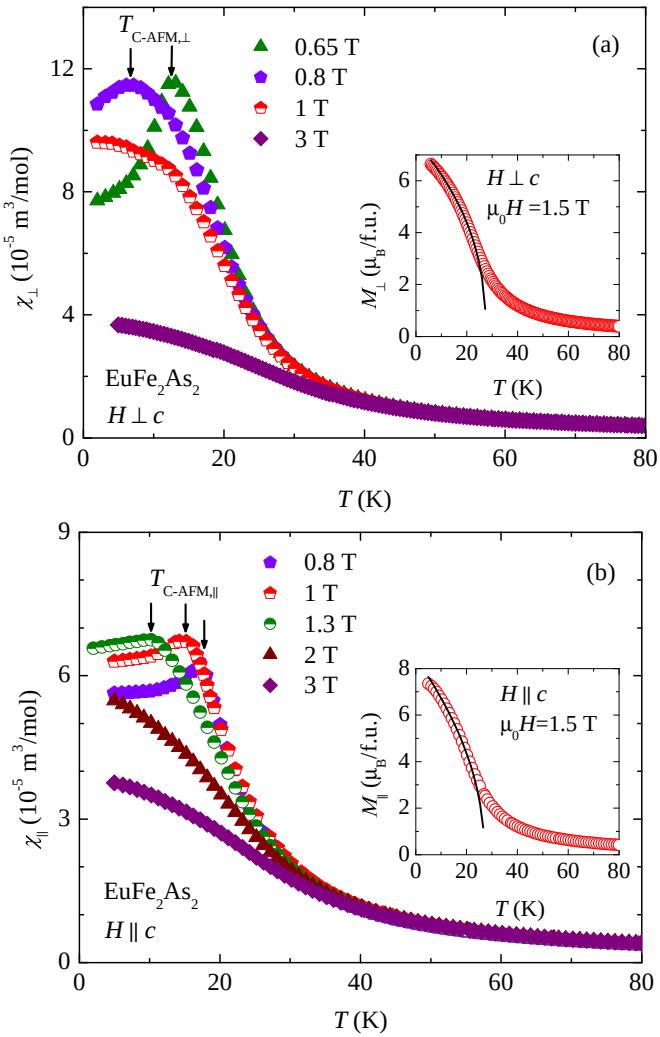


FIG. 3: (Color online) Temperature dependence of the magnetic susceptibility measured at fixed magnetic fields of single-crystal $EuFe_2As_2$ for $H \perp c$ (a) and $H \parallel c$ (b). The arrows mark the canted antiferromagnetic ordering temperature $T_{\mathrm{C-AFM}}$ of the $Eu^{2+}$ moments in low fields. $T_{\mathrm{C-AFM},\perp}$ and $T_{\mathrm{C-AFM},\parallel}$ refer to the C-AFM ordering temperatures for $H \perp c$ and $H \parallel c$, respectively. The insets illustrate the determination of $T_{\mathrm{C}}$ using the power law given in Eq. (3).

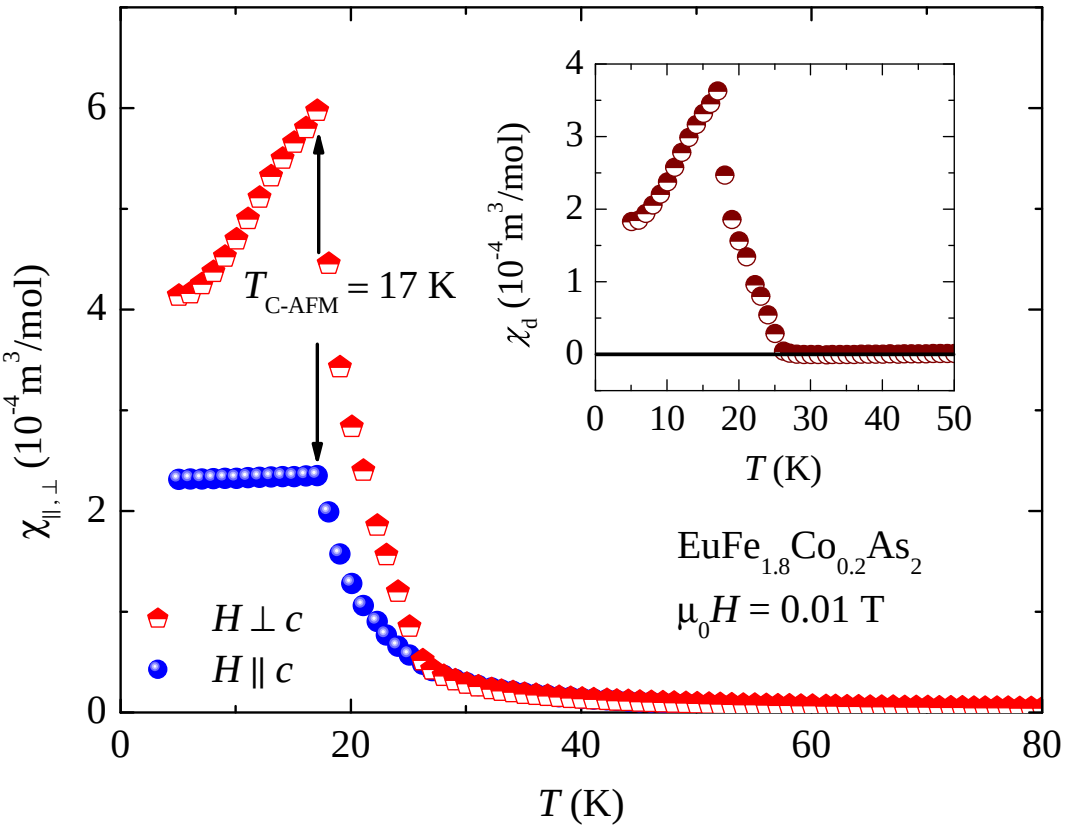


FIG. 4: (Color online) Temperature dependence of the magnetic susceptibility measured in a field of $\mu_0 H = 0.01$ T of single-crystal $EuFe_{1.8}Co_{0.2}As_2$ for $H \perp c$ and $H \parallel c$. The arrows mark the canted antiferromagnetic ordering temperature $T_{C-AFM} \simeq 17$ K of the $Eu^{2+}$ moments. In the inset the difference between the susceptibilities for the two different field configurations ($\chi_d = \chi_\perp - \chi_\parallel$) is plotted as a function of temperature.

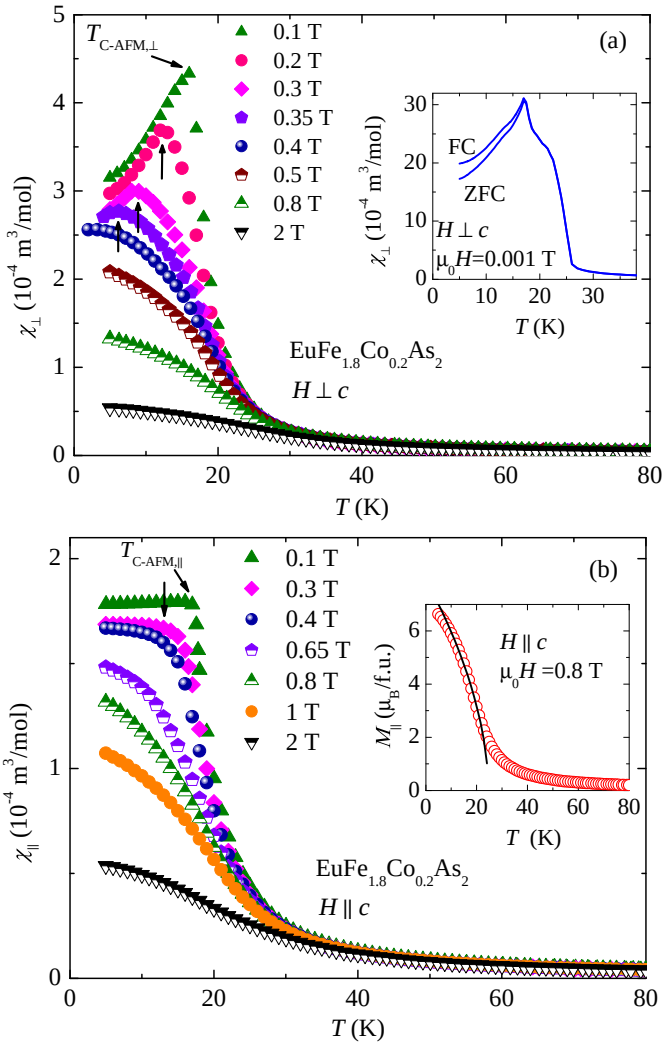


FIG. 5: (Color online) Temperature dependence of the ZFC magnetic susceptibility measured at various fixed magnetic fields of single-crystal $EuFe_{1.8}Co_{0.2}As_2$ for $H \perp c$ (a) and $H \parallel c$ (b). The arrows mark the canted antiferromagnetic ordering temperature $T_{\mathrm{C-AFM}}$ of the $Eu^{2+}$ moments in low magnetic fields. $T_{\mathrm{C-AFM},\perp}$ and $T_{\mathrm{C-AFM},\parallel}$ refer to the C-AFM ordering temperatures for $H \perp c$ and $H \parallel c$, respectively. In the inset of (a) $\chi_\perp(T)$ for FC and ZFC in an applied field of $\mu_0 H = 0.001$ T is plotted. The inset of (b) shows the approximation of $M_\parallel(T)$ in $\mu_0 H = 0.8$ T by the power law (solid curve) given in Eq. (3).

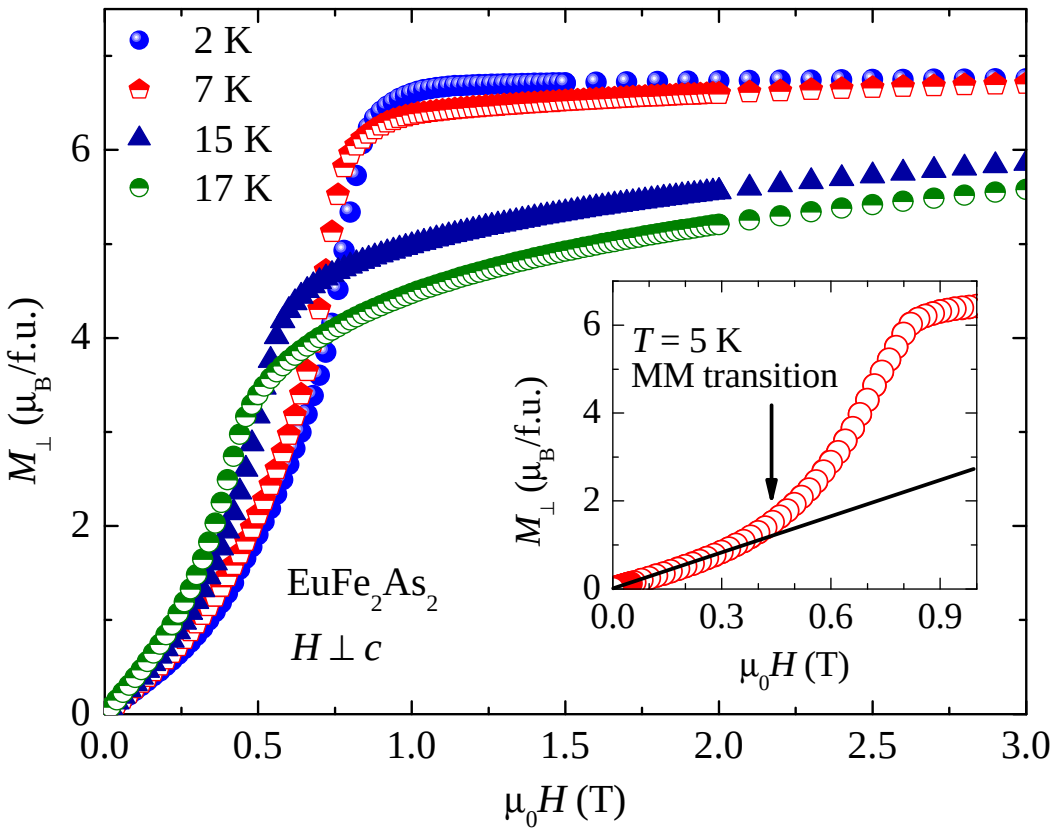


FIG. 6: (Color online) Field dependence of the magnetization at various temperatures of single-crystal $EuFe_2As_2$ for $H \perp c$. The inset shows the low field $M_\perp$ data at 5 K, illustrating the metamagnetic (MM) transition marked by the arrow.

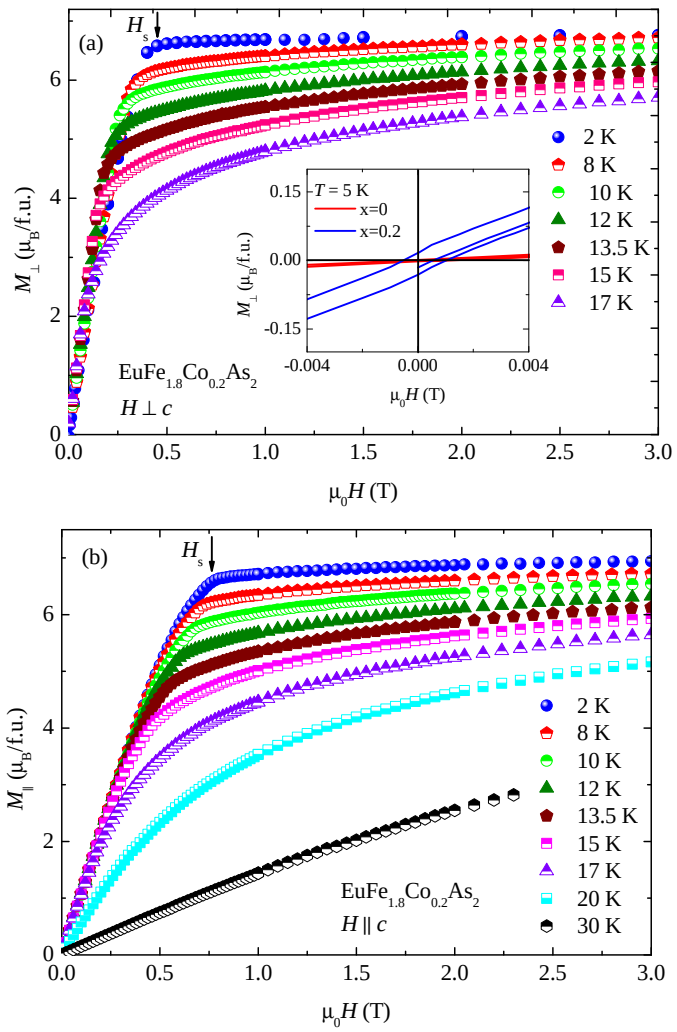


FIG. 7: (Color online) Field dependence of the magnetization at low temperatures of single-crystal $EuFe_{1.8}Co_{0.2}As_2$ for $H \perp c$ (a) and $H \parallel c$ (b). The saturation field $H_s$ at 2 K is marked by arrows. The inset of (a) shows the field dependence of $M_\perp$ for $EuFe_2As_2$ and $EuFe_{1.8}Co_{0.2}As_2$ at 5 K.

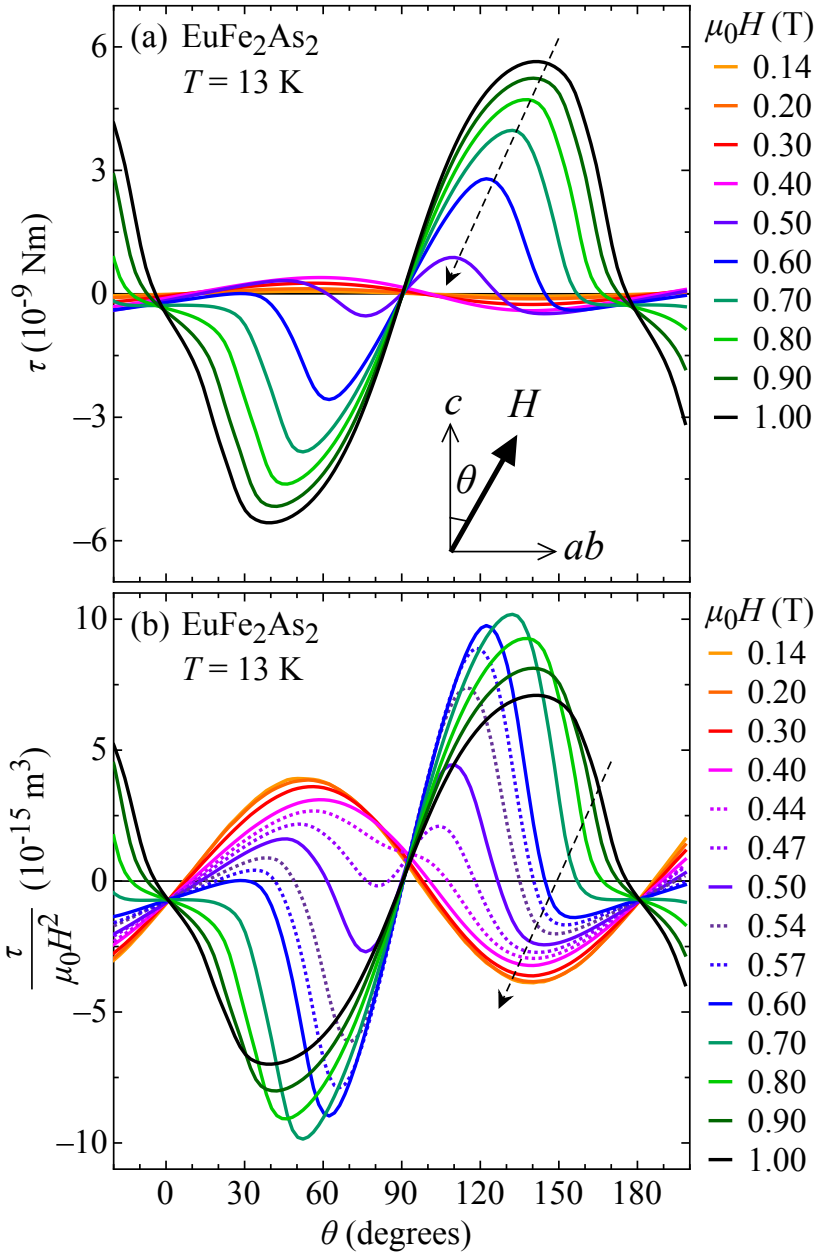


FIG. 8: (Color online) (a) Angular dependent magnetic torque $\tau$ of single-crystal $EuFe_2As_2$ at 13 K in various magnetic fields. For clarity not all measured data are shown. (b) Angular dependence of the quantity $\tau/(\mu_0 H^2)$. The dashed arrows denote the direction of increasing magnetic field.

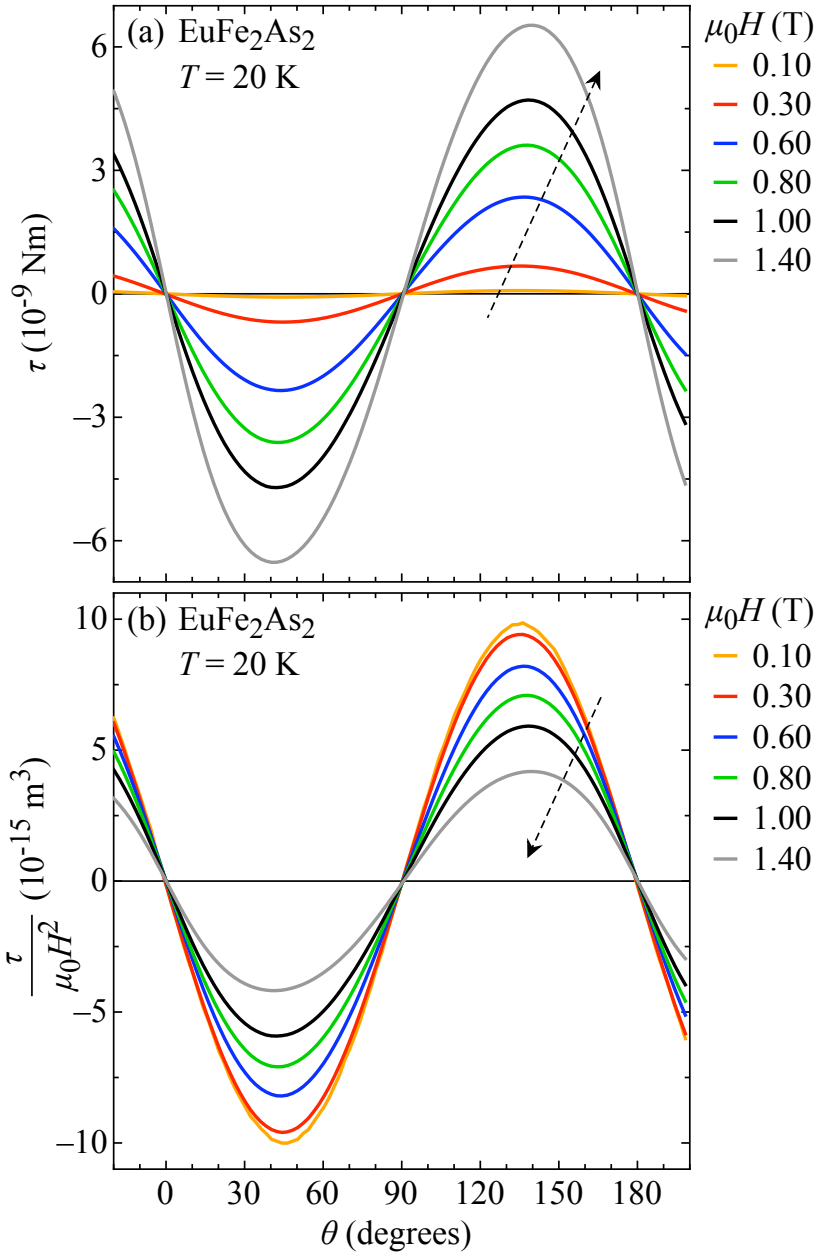


FIG. 9: (Color online) Magnetic torque $\tau$ (a) and the quantity $\tau/(\mu_0 H^2)$ (b) as a function of the angle $\theta$ of single-crystal $EuFe_2As_2$ in various magnetic fields at 20 K. The dashed arrows denote the direction of increasing magnetic field.

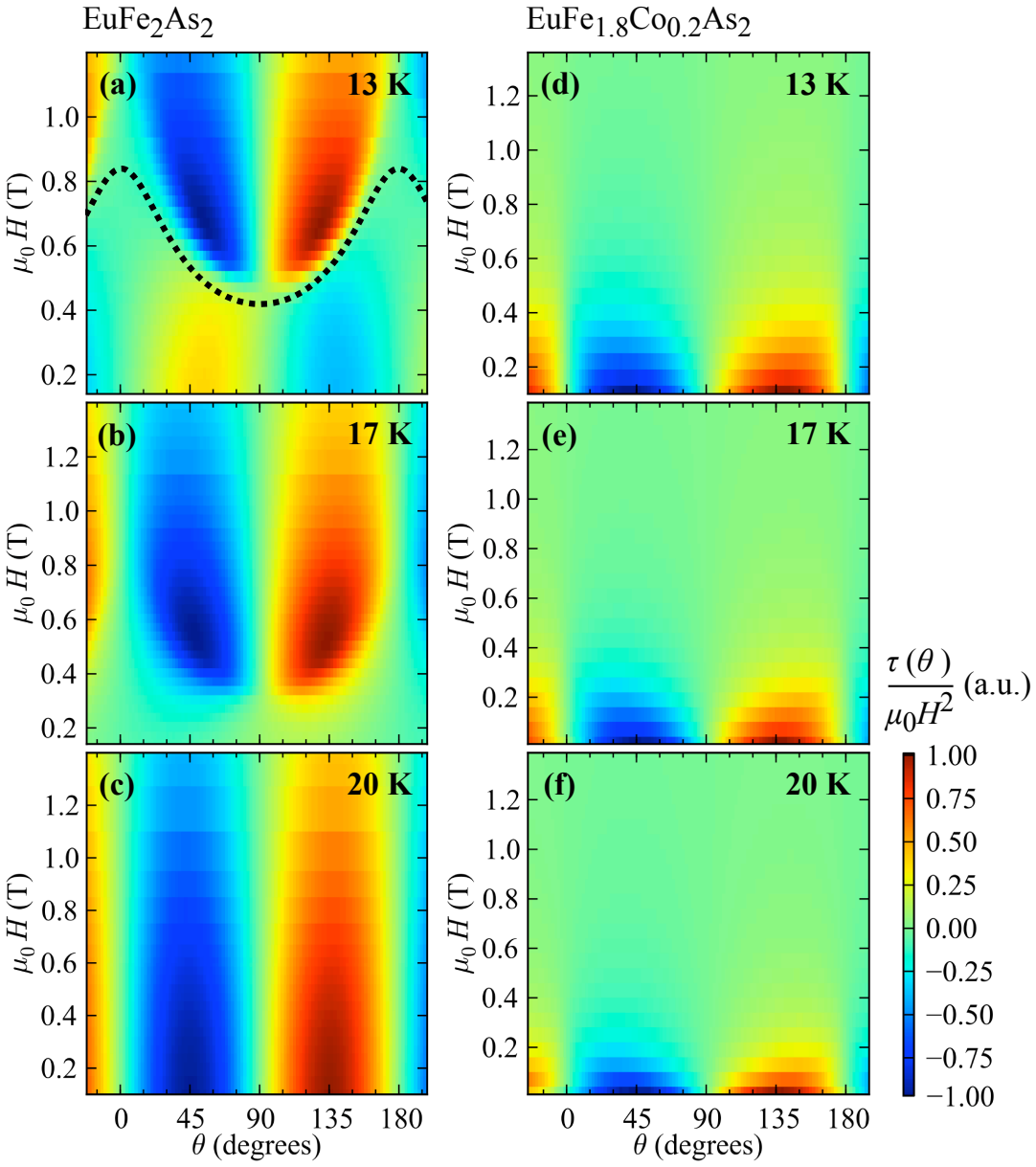


FIG. 10: (Color online) Color map of $\tau/(\mu_0 H^2)$ (in a.u.) for $EuFe_2As_2$ and $EuFe_{1.8}Co_{0.2}As_2$ as a function of angle $\theta$ and field $H$ for $T = 13$ K, 17 K and 20 K. The dotted line in (a) is a fit according to Eq. (6). Panels (a), (b), and (c) are the data for $EuFe_2As_2$ at 13 K, 17 K, and 20 K, respectively, whereas (d), (e) and (f) are the data for $EuFe_{1.8}Co_{0.2}As_2$ at 13 K, 17 K, and 20 K, respectively.

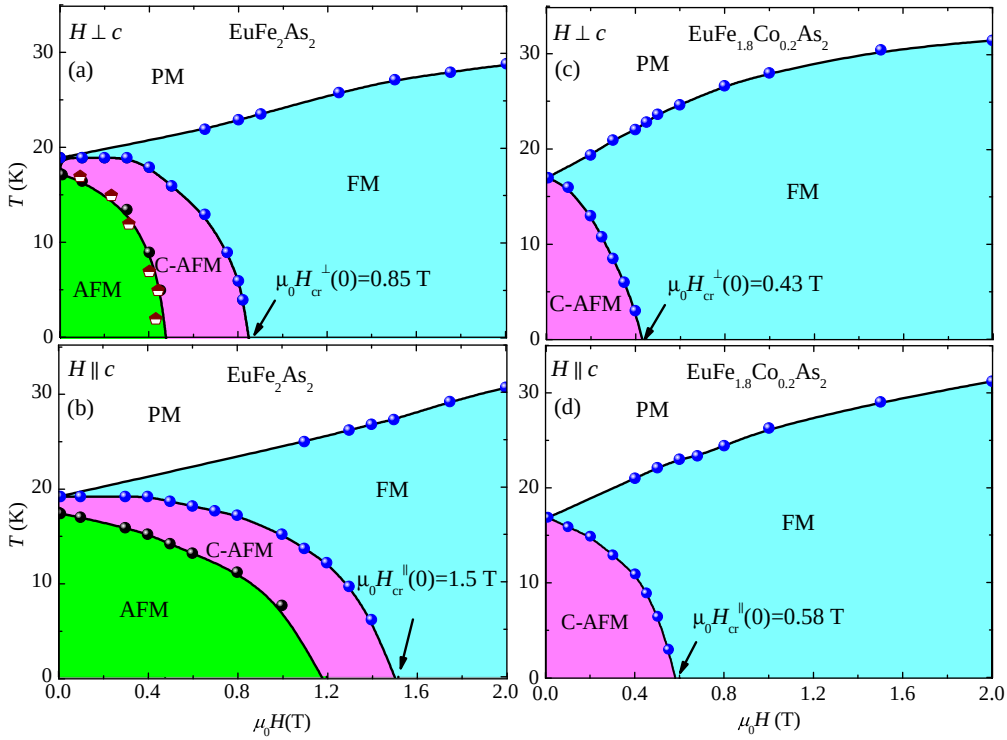


FIG. 11: (Color online) Magnetic phase diagrams of single-crystal $EuFe_2As_2$ (a and b) and single-crystal $EuFe_{1.8}Co_{0.2}As_2$ (c and d) for $H \perp c$ and for $H \parallel c$. The various phases in the phase diagrams are denoted as follows: paramagnetic (PM), antiferromagnetic (AFM), canted antiferromagnetic (C-AFM), ferromagnetic (FM). The filled and open symbols are from the susceptibility and field dependent magnetization measurements, respectively. The solid lines are guides to the eyes.